Title

Distinct stem cell myeloproliferative/T lymphoma syndromes induced by ZNF198-FGFR1 and BCR-FGFR1 fusion genes from 8p11 translocations

Journal

Cancer Cell, 5(3)

ISSN

1535-6108

Authors

Roumiantsev, Sergei
Krause, Daniela S
Neumann, Carola A
et al.

Publication Date

2004-03-01

DOI

10.1016/s1535-6108(04)00053-4

Distinct stem cell myeloproliferative/T lymphoma syndromes induced by *ZNF198-FGFR1* and *BCR-FGFR1* fusion genes from 8p11 translocations

Sergei Roumiantsev,[1,8] Daniela S. Krause,[2,8] Carola A. Neumann,[3] Christopher A. Dimitri,[4] Frances Asiedu,[2] Nicholas C.P. Cross,[5,6] and Richard A. Van Etten[7,*]

[1]Children's Hospital, 330 Longwood Avenue, Boston, Massachusetts 02115
[2]CBR Institute for Biomedical Research, 200 Longwood Avenue, Boston, Massachusetts 02115
[3]Department of Cancer Biology, Dana-Farber Cancer Institute, 44 Binney Street, Boston, Massachusetts 02115
[4]Department of Cell Biology, Harvard Medical School, 240 Longwood Avenue, Boston, Massachusetts 02115
[5]Wessex Regional Genetics Laboratory, Salisbury District Hospital, Salisbury, Wilts SP2 8BJ, United Kingdom
[6]Human Genetics Division, University of Southampton School of Medicine, Southampton S016 6YD, United Kingdom
[7]Molecular Oncology Research Institute, Tufts-New England Medical Center, Boston, Massachusetts 02111
[8]These authors contributed equally to this work
*Correspondence: rvanetten@tufts-nemc.org

Summary

8p11 myeloproliferative syndrome (EMS) is a hematopoietic stem cell disorder characterized by myeloid hyperplasia and non-Hodgkin's lymphoma with chromosomal translocations fusing several genes, most commonly *ZNF198*, to fibroblast growth factor receptor-1 (*FGFR1*). However, patients with *BCR-FGFR1* fusion present with typical chronic myeloid leukemia (CML). We demonstrate that *ZNF198-FGFR1* induces EMS-like disease in mice, with myeloproliferation and T lymphoma arising from common multipotential progenitors. Mutation of FGFR1 Tyr766 attenuates both myeloid and lymphoid diseases, identifying phospholipase C-γ1 as a downstream effector. Bcr-FGFR1 binds Grb2 via Bcr Tyr177 and induces CML-like leukemia in mice, whereas Bcr-FGFR1/Y177F lacks Grb2 binding and causes EMS-like disease. These results implicate different signaling pathways originating from both kinase and fusion partner in the pathogenesis of CML and EMS.

Introduction

The concept of molecularly targeted therapy for cancer became reality with the introduction of imatinib mesylate (Gleevec, formerly STI-571) for the treatment of chronic myeloid leukemia (CML). Imatinib is a small molecule inhibitor of the Abl, platelet-derived growth factor β receptor, and Kit tyrosine kinases that is remarkably effective for induction of hematologic and cytogenetic remissions in chronic phase CML patients (Kantarjian et al., 2002). The rationale for targeting Abl in CML came in part from the demonstration that expression of the *BCR-ABL* fusion gene in bone marrow caused fatal myeloproliferative disease in mice that closely resembled CML (Daley et al., 1990), implicating the Bcr-Abl tyrosine kinase as the direct cause of CML. The success of imatinib in CML illustrates that development of accurate animal models for other human leukemias will be an important step in the identification and validation of potential molecular drug targets. An animal model also provides an avenue to study the pathophysiology of the disease and a platform for developing and testing targeted therapies.

The 8p11 myeloproliferative syndrome (EMS, also known as stem cell leukemia/lymphoma syndrome) is a distinct hematologic disorder characterized by myeloid hyperplasia, eosinophilia, and lymphoblastic lymphoma associated with balanced chromosomal translocations involving 8p11 (Inhorn et al., 1995; Macdonald et al., 1995). The myeloid hyperplasia has some similarity to CML, with overproduction of myeloid cells that retain the capacity to differentiate, but lacks basophilia and tends to progress to acute myeloid leukemia within 1 to 2 years of diagnosis. About 70% of EMS patients present with or develop high-grade non-Hodgkin's lymphoblastic lymphoma, predominantly of a primitive T cell phenotype. Both myeloid and lymphoma cells share the 8p11 translocation, demonstrating that the disease originates from a hematopoietic stem cell. The

SIGNIFICANCE

Tyrosine kinases are increasingly important targets for the development of drugs for treatment of hematologic malignancies and solid tumors, but monotherapy with kinase inhibitors may lead to resistance. Using a mouse retroviral bone marrow transplant model, we demonstrate that the ZNF198-FGFR1 fusion kinase is the direct cause of human 8p11 myeloproliferative syndrome, validating it as a therapeutic target, and identify phospholipase C-γ as a critical downstream pathway whose blockade may complement kinase inhibitor therapy. In contrast, the Bcr-FGFR1 fusion kinase from patients with t(8;22) induces chronic myeloid leukemia-like disease through a pathway involving Grb2. This model system will be useful for further studies of the pathophysiology of 8p11 syndrome and for developing and testing molecularly targeted therapies.

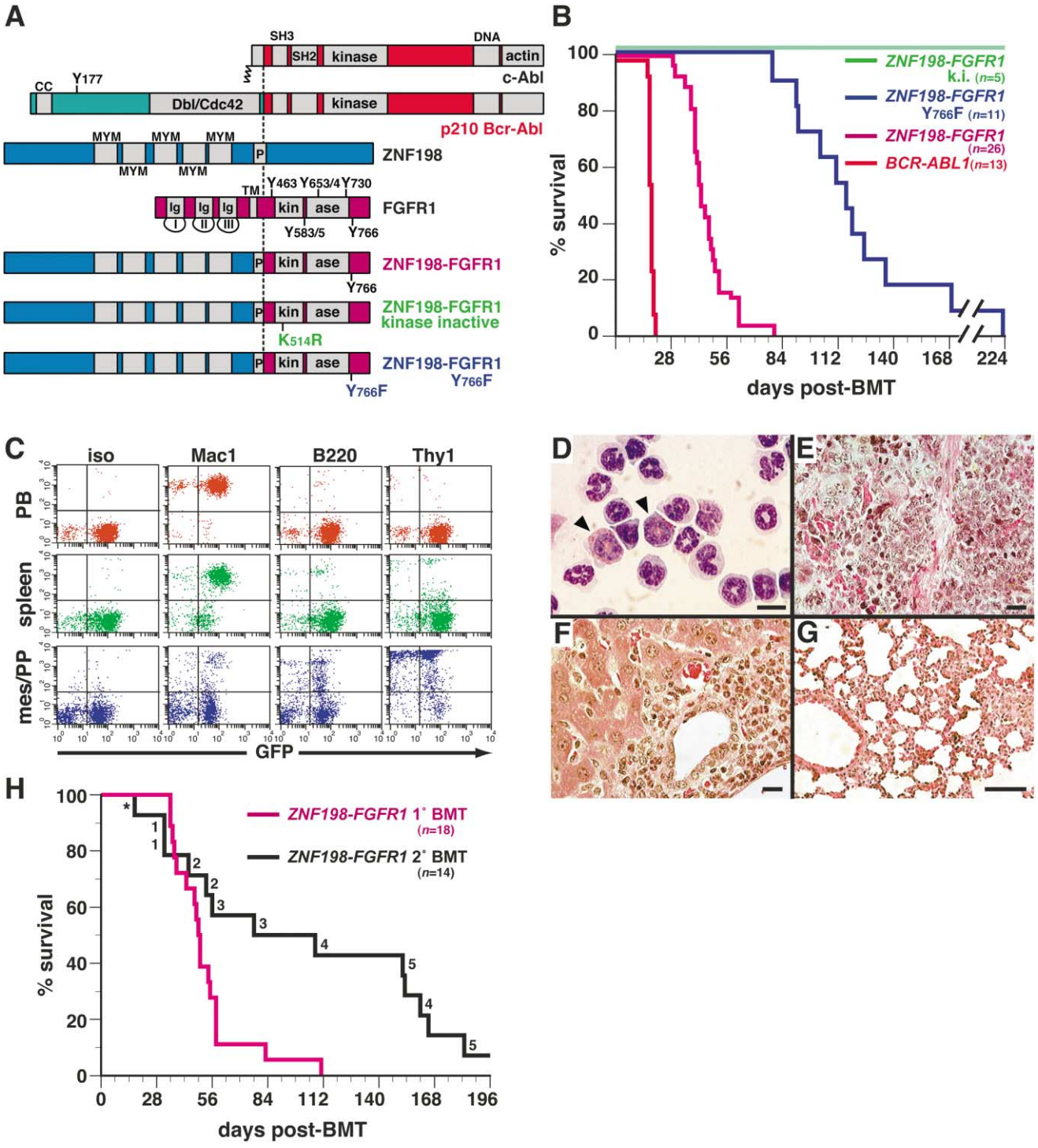

Figure 1. *ZNF198-FGFR1* induces distinct MPD in mice

A: Schematic of (top to bottom) c-Abl, p210 Bcr-Abl, ZNF198, FGFR1, and ZNF198-FGFR1 polypeptides, including ZNF198-FGFR1 kinase-inactive (K514R) and PLC-γ_1 binding site (Y766F) mutants. Domains indicated by gray boxes include SH3, SH2, kinase, DNA binding, and actin binding domains in Abl, coiled-coil (CC) domain, Tyr177 Grb2 binding site, and Dbl/Cdc42 homology domain in Bcr, zinc finger (MYM) repeats (Reiter et al., 1998) and proline-rich (P) dimerization domain (Xiao et al., 2000) in ZNF198, and extracellular Ig repeats, transmembrane (TM) domain, split kinase domain, and seven intracellular tyrosine autophosphorylation sites (Mohammadi et al., 1996) in FGFR1 (numbered according to their position in normal FGFR1). The point of fusion is indicated by the vertical dotted line.

B: Kaplan-Meier-style survival curve for recipients of bone marrow transduced with *BCR-ABL* (red, n = 13), *ZNF198-FGFR1* (magenta, n = 26), *ZNF198-FGFR1* Y766F mutant (blue, n = 11), and *ZNF198-FGFR1* kinase-inactive (k.i.) mutant (green, n = 5). The difference in survival between any of the individual arms is highly significant ($p < 0.0001$, Mantel-Cox test).

C: Flow cytometric plots of peripheral blood (PB, in red), spleen (in green), and mesenteric lymph node/Peyer's patch cells (mes/PP, blue) from a representative mouse transplanted with *ZNF198-FGFR1*-transduced marrow, sacrificed 42 days posttransplant with a peripheral blood leukocyte count of

Table 1. Clinicopathological features of leukemias induced by fusion tyrosine kinases

Oncogene	Median survival (days)	PB WBC[a] (death)	Spleen weight (g)	Liver histiocytic infiltrates	Lung myeloid infiltration/hemorrhage	T lymphoma	
						Intestine	Thymus
p210 *BCR-ABL*	17	326 ± 79	0.80 ± 0.03	+	++	−	−
ZNF198-FGFR1	42	44 ± 21[b]	0.36 ± 0.05[b]	−	+	+	−
ZNF198-FGFR1 Y766F	116	27 ± 15	0.49 ± 0.12	−	−	+	+
BCR-FGFR1	14	220 ± 55	0.39 ± 0.02	+	++	−	−
BCR-FGFR1 Y177F	39	12 ± 4[c]	0.30 ± 0.03	++	−	+	−

+, present; ++, extensive; −, absent.
[a] Peripheral blood leukocyte count.
[b] Significantly different from corresponding *BCR-ABL* values ($p < 0.001$, unpaired t test).
[c] Significantly different from *BCR-FGFR1* ($p < 0.01$, unpaired t test).

translocation partner can be derived from several different chromosomes including 6q27, 9q33, 11p15, 12q15, 13q12, 17q25, and 19q13 (Macdonald et al., 2002).

The breakpoint of the most common EMS-associated translocation, t(8;13)(p11;q12), was molecularly cloned in 1998 and shown to fuse a novel gene on 13q12, *ZNF198* (also called *FIM* or *RAMP*), to the fibroblast growth factor receptor-1 (*FGFR1*) gene on 8p11 (Popovici et al., 1998; Reiter et al., 1998; Smedley et al., 1998; Xiao et al., 1998). Subsequently, breakpoints of the t(6;8), t(8;9), and t(8;19) translocations were identified and found to fuse the *FOP* gene on 6q27 (Popovici et al., 1999), the *CEP110* gene on 9q33 (Guasch et al., 2000), and an endogenous human retroviral sequence on 19q13 (Guasch et al., 2003), respectively, to *FGFR1*. The resulting chimeric genes produce fusions of distinct amino-terminal partner proteins with the cytoplasmic tyrosine kinase domain of FGFR1. Recently, several patients with t(8;22) have been described with 8p11 translocations involving the *BCR* gene on 22q11, identifying Bcr as a fifth fusion partner for FGFR1 (Demiroglu et al., 2001; Fioretos et al., 2001). Interestingly, these patients present with myeloproliferative disease and basophilia but without lymphoma, and hence more closely resemble typical Ph^+ CML rather than EMS, suggesting that the leukemia phenotype might be influenced by the identity of the FGFR1 fusion partner.

The *ZNF198* gene is ubiquitously expressed and encodes a protein with five novel zinc finger repeats that is localized to the cell nucleus and nucleolus (Ollendorff et al., 1999). The ZNF198-FGFR1 and Bcr-FGFR1 fusion proteins are cytoplasmically localized, constitutively active tyrosine kinases that transform Ba/F3 cells to become independent of interleukin-3 for survival and proliferation (Demiroglu et al., 2001; Ollendorff et al., 1999; Popovici et al., 1998; Smedley et al., 1999; Xiao et al., 1998). ZNF198-FGFR1 transforming activity requires a novel proline-rich oligomerization domain in ZNF198 (Xiao et al., 2000), suggesting that FGFR1 fusion partners induce constitutive FGFR1 tyrosine kinase activity through self-association, analogous to the activation of Abl by the coiled-coil oligomerization domain in Bcr. Studies in Ba/F3 cells demonstrate that in contrast to Bcr-Abl, ZNF198-FGFR1 and Bcr-FGFR1 are resistant to imatinib but sensitive to a specific FGFR1 kinase inhibitor (Smedley et al., 1999). Otherwise, no significant differences in oncogenic activity between Bcr-Abl and the various FGFR1 fusion kinases have been identified.

An understanding of the pathogenesis of leukemias associated with activated forms of FGFR1 requires expression of 8p11 fusion genes in the hematopoietic system. Here, we tested the leukemogenic activity of *ZNF198-FGFR1* and *BCR-FGFR1* oncogenes in a murine bone marrow transduction/transplantation model system. We demonstrate that *ZNF198-FGFR1* and *BCR-FGFR1* induce distinct hematologic disease in mice through different signaling pathways originating from both the partner protein and the kinase domain.

Results

ZNF198-FGFR1 induces myeloproliferative disease and T lymphoma in mice

We transduced bone marrow from 5-fluorouracil-treated Balb/c donor mice with retrovirus coexpressing fusion tyrosine kinases (Figure 1A) and green fluorescent protein (GFP) via an internal ribosome entry site (Schwaller et al., 1998), and transplanted the marrow into lethally irradiated syngeneic recipient mice. As described previously (Li et al., 1999), recipients of marrow transduced with p210 *BCR-ABL* developed rapidly fatal myeloproliferative disease (MPD) resembling human CML (Figure 1B and Table 1), with massive expansion of maturing myeloid cells and infiltration of spleen, liver, and lungs (Million et al., 2002, and data not shown). In contrast, recipients of *ZNF198-FGFR1*-transduced marrow

$53.2 \times 10^3/\mu l$ and spleen weight of 0.33 g. Cells were stained with PE-conjugated (*y* axis) isotype control antibody (iso) or antibodies against Mac-1, B220, or Thy-1. Expression levels of GFP are shown along the *x* axis; cells from an untransplanted Balb/c mouse were localized to the left lower quadrant (>99%, data not shown). Note GFP^+ spleen cells expressing B220 or Thy-1 indicative of multilineage repopulation.
D–G: Chronic MPD in recipients of *ZNF198-FGFR1*-transduced marrow. **D:** Wright-Giemsa-stained peripheral blood with several eosinophils (arrowheads). **E:** Hematoxylin and eosin (H&E)-stained spleen. **F:** H&E-stained liver. **G:** H&E-stained lung. Scale bars: 10 μm (**D**), 20 μm (**E** and **F**), 100 μm (**G**).
H: Survival curve of primary recipients of *ZNF198-FGFR1*-transduced bone marrow (magenta, n = 18) and of lethally irradiated secondary recipients of BM and/or spleen from these diseased primary mice (black, n = 14). The majority of secondary recipients had evidence of chronic MPD and succumbed to T lymphoma. Pairs of recipients transplanted with cells from the same primary donor are indicated by numbers. The animal indicated by the asterisk died on day 17 posttransplant with pancytopenia and likely failed to engraft.

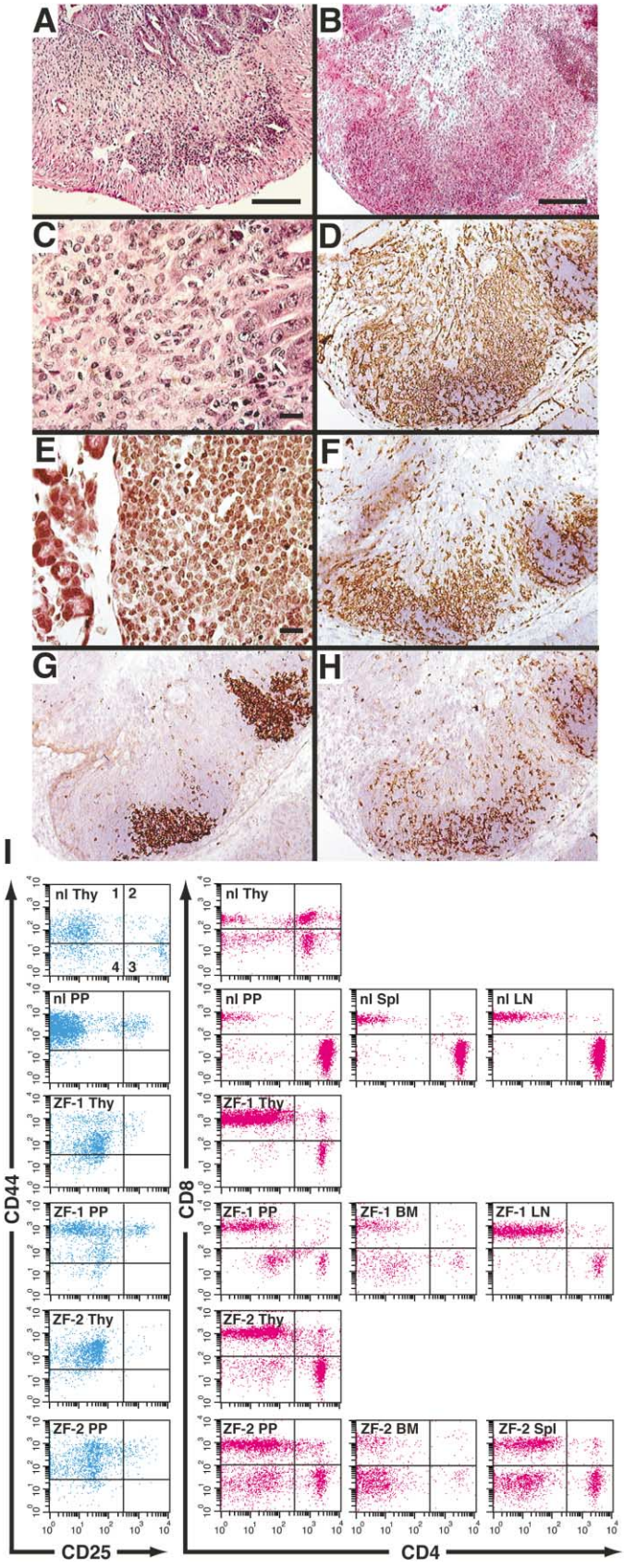

survived significantly longer (Figure 1B) and succumbed to distinct disease (Table 1). All *ZNF198-FGFR1* recipients developed MPD as evidenced by leukocytosis, splenomegaly, and increased GFP^+ Mac-1^+ cells in peripheral blood, spleen, and bone marrow (Figure 1C and data not shown), but the circulating myeloid cells were more mature than in *BCR-ABL*-induced MPD (Li et al., 2001b), with few myelocytes and promyelocytes (Figure 1D). About 20% (9/44) of *ZNF198-FGFR1* recipients had eosinophilia (defined as >5% eosinophils in peripheral blood or bone marrow), while eosinophilia was not observed in *BCR-ABL* recipients (Li et al., 2001b) (and data not shown). Spleens demonstrated follicular disruption by maturing myeloid and erythroid cells and increased fibrosis (Figure 1E). Livers exhibited perivenular neutrophil infiltration (Figure 1F) but lacked the erythroid and histiocytic infiltrates characteristic of *BCR-ABL*-induced CML-like disease (Million et al., 2002). There was modest pulmonary myeloid cell infiltration (Figure 1G), in contrast to the extensive infiltrates and hemorrhages that are the cause of death in *BCR-ABL* recipients.

Patients with the *ZNF198-FGFR1* fusion usually develop non-Hodgkin's lymphoma, predominantly immature T lymphoblastic lymphoma, in addition to MPD (Inhorn et al., 1995; Macdonald et al., 1995). Significantly, all murine *ZNF198-FGFR1* recipients also developed T cell lymphoma principally involving the small intestine. Grossly, the bowel was swollen with prominent serosal nodules accompanied by mesenteric and celiac lymphadenopathy. Some mice had minimal peripheral lymph node enlargement but thymuses were normal. Microscopically, the disease originated in hyperplastic Peyer's patches, with disruption of normal follicles and infiltration of submucosal and intervillous spaces by large cells with immature nuclei and eosinophilic cytoplasm (Figures 2A–2C). This led to the loss of the entire intestinal epithelium in some areas (data not shown) and

Figure 2. Characterization of *ZNF198-FGFR1*-induced T lymphoma

A–H: Intestinal T cell lymphoma in *ZNF198-FGFR1* recipients. **A:** H&E-stained neoplastic Peyer's patch from small intestine, demonstrating disruption of normal follicles (bottom) with submucosal and intervillous invasion by malignant lymphoblasts (top). **B:** H&E-stained frozen section of malignant Peyer's patch. **C:** Closeup view of Peyer's patch in **A**, demonstrating infiltration of sub- and intervillous spaces by immature lymphoblasts with large nuclei and eosinophilic cytoplasm. **D:** Anti-Thy-1 immunoperoxidase staining of Peyer's patch from **B**, showing strong immunoreactivity of infiltrating cells. **E:** H&E-stained peripancreatic lymph node demonstrating replacement with lymphoblastic cells. Immunohistochemical staining demonstrated the majority of the cells were Thy-1^+ with variable expression of CD8 (data not shown). **F–H:** Anti-CD8 (**F**), anti-B220 (**G**), and anti-CD4 (**H**) immunoperoxidase staining of the Peyer's patch from **B**. Staining with antibody directed against GFP showed a similar pattern to **D** (data not shown). Staining of Peyer's patches from control mice demonstrated well-formed follicles that were GFP^- and predominantly $B220^+$ with a peripheral Thy-1^+/$CD4^+$ population and no staining of submucosal and intervillous areas, while staining of normal or malignant tissue with isotype control antibody was negative (data not shown). Scale bars: 100 μm (**A**, **B**, **D**, **F**, and **G**), 20 μm (**C** and **E**).
I: Flow cytometric characterization of GFP^+ Thy1^+ cells from diseased mice. The GFP^+ Thy1^+ cell population from thymus (Thy), Peyer's patches (PP), peripheral lymph nodes (LN), bone marrow (BM), or spleen (Spl) of a normal Balb/c mouse (nl, top two rows) or two representative mice with *ZNF198-FGFR1*-induced EMS-like disease (ZF-1 and ZF-2, bottom four rows) was analyzed for expression of CD44 and CD25 (blue panels) or CD4 and CD8 (red panels) as described in the Experimental Procedures. The quadrants comprising the DN1-DN4 populations in normal thymus are indicated by the respective numbers.

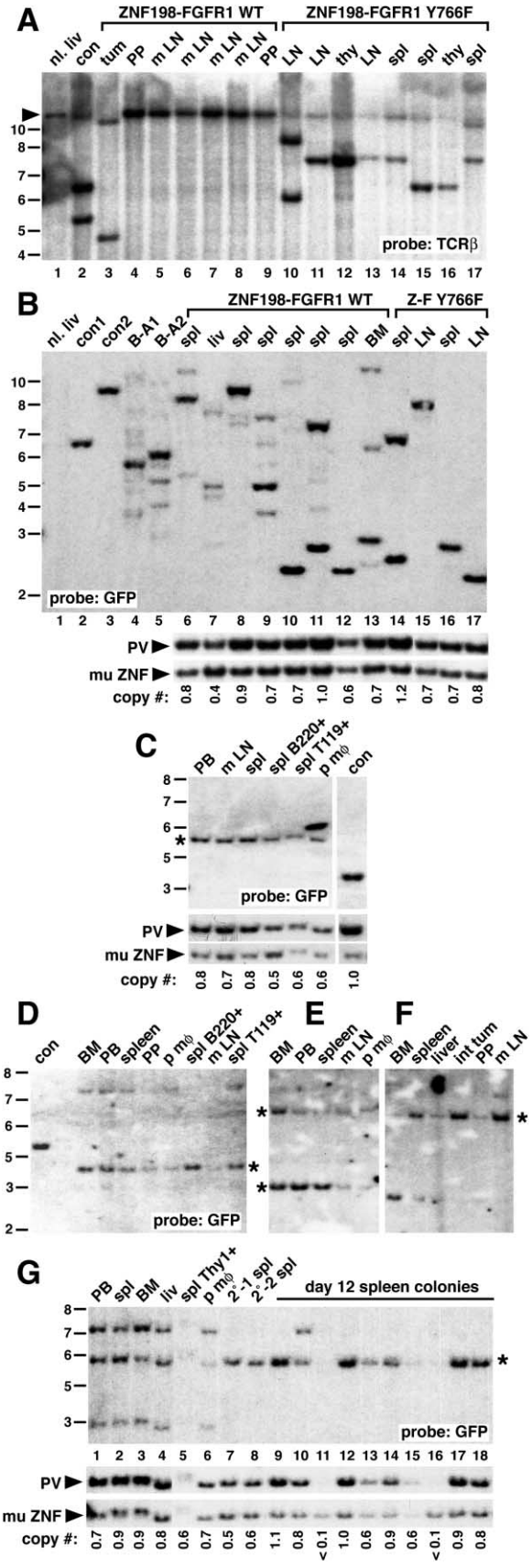

was the likely cause of death in all *ZNF198-FGFR1* recipients. The lymphomas were Thy-1$^+$ with variable expression of CD4 and CD8 but negative for TdT, B220, and myeloid markers (Figures 2D and 2F–2H, and data not shown), and most had germline T cell receptor β (TCRβ) genes (Figure 3A), indicative of an early T cell phenotype. GFP$^+$ Thy1$^+$ lymphoblastic cells were also found in enlarged mesenteric and peripancreatic lymph nodes (Figures 1C and 2E).

Figure 3. *ZNF198-FGFR1*-induced MPD and T lymphoma arise from a common multipotential progenitor

A: TCRβ gene rearrangements in *ZNF198-FGFR1*-induced T lymphomas. Genomic DNA from normal liver (nl. liv, lane 1), a control *BCR-ABL*-transformed T cell line (con, lane 2), and primary T lymphoma cells from several individual *ZNF198-FGFR1* wild-type (WT, lanes 3–9) and *ZNF198-FGFR1* Y766F (lanes 10–17) recipient mice were digested with Bgl II and hybridized with a TCRβ probe (Million and Van Etten, 2000). The position of the germline band is indicated by the arrowhead. Paired samples in lanes 4/5, 8/9, 11/12, 13/14, and 15/16 are from the same mice. Note germline status of TCRβ in 4 of 5 *ZNF198-FGFR1*-induced T lymphomas but clonal rearrangements in all *ZNF198-FGFR1 Y766F*-induced lymphomas. Tum, tumor; PP, Peyer's patch; m LN, mesenteric lymph node/mass; LN, peripheral lymph node; thy, thymus; spl, spleen.

B: *ZNF198-FGFR1*-induced disease is oligo- to monoclonal. Genomic DNA from the indicated tissues (nomenclature as above; BM = bone marrow) was analyzed by hybridization with a *GFP* probe to detect distinct bands from each proviral integration site. con1 and con2 are control DNAs from Ba/F3 cell lines each containing a single *BCR-ABL* provirus, while B-A1 and B-A2 are spleen DNAs from two different mice with *BCR-ABL*-induced MPD. Lanes 6–13 and 14–17 are DNAs from the indicated tissues of mice with *ZNF1980FGFR1* WT- and Y766F-induced disease, respectively. The blot was stripped and rehybridized with a *ZNF198* probe (bottom panels) that detects a common 3.5 kb band from all proviruses (PV, arrowhead) and the endogenous murine *ZNF198* gene (mu ZNF, arrowhead), allowing determination of the average number of proviruses per cell (copy number) (Li et al., 1999), which was near single-copy for all mice (corresponding to a value of 1.0). The bands in lanes 10 and 12, though of similar size, originate from different integration sites as determined by a blot with EcoRI-digested DNA (data not shown).

C–G: The cell initiating *ZNF198-FGFR1*-induced EMS-like disease has multilineage repopulating ability and generates day 12 spleen colonies. Genomic DNA from purified cells from different hematopoietic lineages from five different mice with *ZNF198-FGFR1*-induced EMS-like disease was analyzed as in **B**. The same proviral clone was present at near single-copy levels in peripheral blood neutrophils (PB), peritoneal macrophages (p mϕ), spleen erythroid (spl T119+) and B lymphoid (spl B220+) cells, and T lymphoma cells from mesenteric lymph node/mass (m LN) and/or malignant Peyer's patch tissue (PP) from one such animal (**C**). Proviral copy number (bottom panels) was determined by hybridization with a *ZNF198* probe as in **B**; control genomic DNA with a single *ZNF198-FGFR1* provirus is at the right (con). Likewise, a common proviral clone (asterisk) was present at high levels in bone marrow (BM) and peripheral blood myeloid cells, peritoneal macrophages, total spleen and splenic B lymphoid and erythroid cells, and Peyer's patch and mesenteric T lymphoma cells from another diseased mouse (**D**), while one or two proviral clones (asterisks) were shared among myeloid cells (BM, spleen, p mϕ) and T lymphoma from Peyer's patch, mesenteric nodes, or intestinal tumor mass (int tum) in two additional mice (**E** and **F**). In a primary mouse with triclonal EMS-like disease (**E**), the same three clones were observed in several hematopoietic lineages including peripheral blood neutrophils, peritoneal macrophages, and spleen T lymphoid cells (spl Thy-1$^+$; this sample is underloaded but has high total proviral content as determined in the bottom panels). One of the same clones (asterisk) was found in spleens of two secondary recipients of bone marrow from this mouse that developed EMS-like disease and succumbed to T lymphoma (2°-1 and 2°-2) as well as 8 of 10 day 12 spleen colonies isolated from additional secondary recipients (lanes 9–18; lane 10 is likely from an accidental mixture of two colonies). Similar results were observed with 2 additional CFU-S donors (data not shown). DNA size markers (in kb) are on the left.

To define better the T lymphomas induced by *ZNF198-FGFR1*, we characterized GFP$^+$ Thy1$^+$ cells from different tissues from diseased mice by flow cytometry (Figure 2I). The lymphoma cells were recognizable as CD4$^-$ CD8$^-$ (double negative, DN) cells isolated from Peyer's patches (PP) that were predominantly CD44$^+$ CD25$^-$ with a minor population of CD44$^+$ CD25$^+$ cells, corresponding to the DN1 and DN2 subsets of prothymocytes, respectively. In the thymus, which was of normal size and architecture (data not shown), there was a shift in the thymocyte population toward CD4$^+$ or CD8$^+$ single positive (SP) cells and a relative paucity of DN and double positive populations, with the DN population composed predominantly of DN1 cells. The peripheral lymph nodes of diseased mice were generally normal with exclusively SP T cells, but abnormal GFP$^+$ Thy1$^+$ DN1-like cells could be found in several tissues, including bone marrow and spleen, and likely also represented malignant lymphoma. CD8$^+$ cells present in malignant Peyer's patches (Figures 2F and 2I) could represent nonmalignant *ZNF198-FGFR1*-expressing CD8$^+$ cells with polyclonal TCR rearrangements and/or a population of malignant CD8$^+$ cells that progressed beyond the DN stage without TCR rearrangement. These results confirm that the T lymphomas in *ZNF198-FGFR1* recipients have an early prothymocyte phenotype and demonstrate that *ZNF198-FGFR1* expression perturbs but does not block T cell development.

ZNF198-FGFR1-induced EMS-like disease originates from a hematopoietic stem/progenitor cell

In EMS patients, the 8p11 translocation is found in both myeloid cells and the T lymphoma, indicating a stem cell origin (Inhorn et al., 1995; Macdonald et al., 1995). The EMS-like disease induced in mice by *ZNF198-FGFR1* was oligo- to monoclonal (Figure 3B), and the same proviral clone(s) were detected in neutrophils, macrophages, erythroid, B lymphoid, and T lymphoma cells (Figures 3C–3F). In addition, the majority (20/26) of day 12 spleen colonies generated in secondary transplants from several different primary mice with *ZNF198-FGFR1*-induced EMS-like disease contained the *ZNF198-FGFR1* provirus (Figure 3G and data not shown), indicating that the EMS-like disease arose from a cell with capacity to generate an early multipotential myeloid progenitor, CFU-S_{12}. These results demonstrate that, similar to *BCR-ABL*-induced CML-like disease (Li et al., 1999), a common hematopoietic stem/progenitor cell initiates both the MPD and T lymphoma in recipients of *ZNF198-FGFR*-transduced marrow. The EMS-like disease could be adoptively transferred by transplantation of bone marrow and/or spleen from a primary mouse to lethally irradiated recipients (Figure 1H), with secondary recipients developing chronic MPD and succumbing after a variable period to T lymphoma arising from a common clone identified in the primary animal (Figure 3G and data not shown). Collectively, pathologic and molecular analysis of the EMS-like disease induced in mice by *ZNF198-FGFR1* reveals a striking similarity to the human 8p11 syndrome.

The PLC-γ1 binding site at FGFR1 Tyr766 contributes to MPD and T lymphoma induced by ZNF198-FGFR1

Upon ligand-induced dimerization, FGFR1 undergoes autophosphorylation at seven tyrosine residues in the intracellular domain (Mohammadi et al., 1996) (Figure 1A). Phosphorylated Tyr463 and Tyr766 serve as binding sites for the Src homology 2 (SH2) domains of Crk (Larsson et al., 1999) and phospholipase C-γ1 (PLC-γ1) (Mohammadi et al., 1992), respectively, while the pair of tyrosines (653/654) in the activation loop is required for kinase activation (Mohammadi et al., 1996). The function of the other three sites is unknown. We tested the contribution of FGFR1 autophosphorylation sites to transformation of Ba/F3 and NIH 3T3 cells by *ZNF198-FGFR1*, using a stringent single-step assay for IL-3-independent and anchorage-independent growth, respectively. Transformation was abolished by K514R or Y653/654F mutations that eliminate kinase activity, and significantly decreased by mutation of the PLC-γ1 binding site at Tyr766 but not by individual mutation of the other 4 tyrosines (Figure 4A).

To test the role of Tyr766 in leukemogenesis, we transplanted mice with marrow transduced with the *ZNF198-FGFR1* Y766F mutant. Recipients of *ZNF198-FGFR1* Y766F-transduced marrow survived significantly longer than wild-type *ZNF198-FGFR1* recipients, while the kinase-inactive *ZNF198-FGFR1* K514R mutant did not induce disease (Figures 1A and 1B, and Table 1). All *ZNF198-FGFR1* Y766F recipients developed attenuated MPD with lower leukocyte counts compared to wild-type *ZNF198-FGFR1* recipients (Figures 4B and 4C), and ultimately succumbed to oligoclonal T cell leukemia/lymphoma (Figure 3B), with circulating GFP$^+$ Thy-1$^+$ lymphoblasts (Figure 4C) and involvement of the thymus, peripheral lymph nodes (Figure 4D), spleen, and bone marrow in addition to the small bowel and mesentery (data not shown). The T lymphoma had a more mature phenotype than that induced by wild-type *ZNF198-FGFR1*, with coexpression of CD4 and CD8 (Figure 4D) and clonal rearrangements of TCRβ loci (Figure 3A). These results demonstrate that FGFR1 Tyr766 contributes to both the myelo- and lymphoproliferative diseases induced in mice by *ZNF198-FGR*.

We assessed the activation of PLC-γ1 in primary leukemia cells from diseased mice using Western blotting with antibodies specific for phospho-Tyr783 (Figure 4E). Phosphorylation of PLC-γ1 Tyr783 was observed in Ba/F3 cells, T lymphoma cells, and primary myeloid cells expressing wild-type *ZNF198-FGFR1*, but was greatly diminished or absent in *ZNF198-FGFR1* Y766F-expressing cells (Figure 4E). These results demonstrate that FGFR1 Tyr766 is required for activation of PLC-γ1 by *ZNF198-FGR1,* and implicate PLC-γ1 in the pathogenesis of EMS.

BCR-FGFR1 induces fulminant CML-like myeloproliferative disease in mice

Patients with t(8;22) have fusion of *BCR* to *FGFR1* (Figure 5A) and present with typical CML rather than EMS (Demiroglu et al., 2001; Fioretos et al., 2001). Interestingly, *BCR-FGFR1* induced rapidly fatal CML-like MPD in mice, with significantly shortened survival relative to *BCR-ABL* (Figure 5B). Recipients of *BCR-FGFR1*-transduced marrow developed extreme leukocytosis within 14 days posttransplant, while *BCR-ABL*-induced leukocytosis was delayed by several days (Figures 5C and 5D). Similar to *BCR-ABL*, *BCR-FGFR1* recipients succumbed to respiratory insufficiency with extensive infiltration of spleen, liver, and lungs with maturing GFP$^+$ myeloid cells (Figure 5C) and histopathology that was identical to *BCR-ABL*-induced disease (Million et al., 2002), but lacked evidence of lymphoma in the bowel or elsewhere (Table 1 and data not shown).

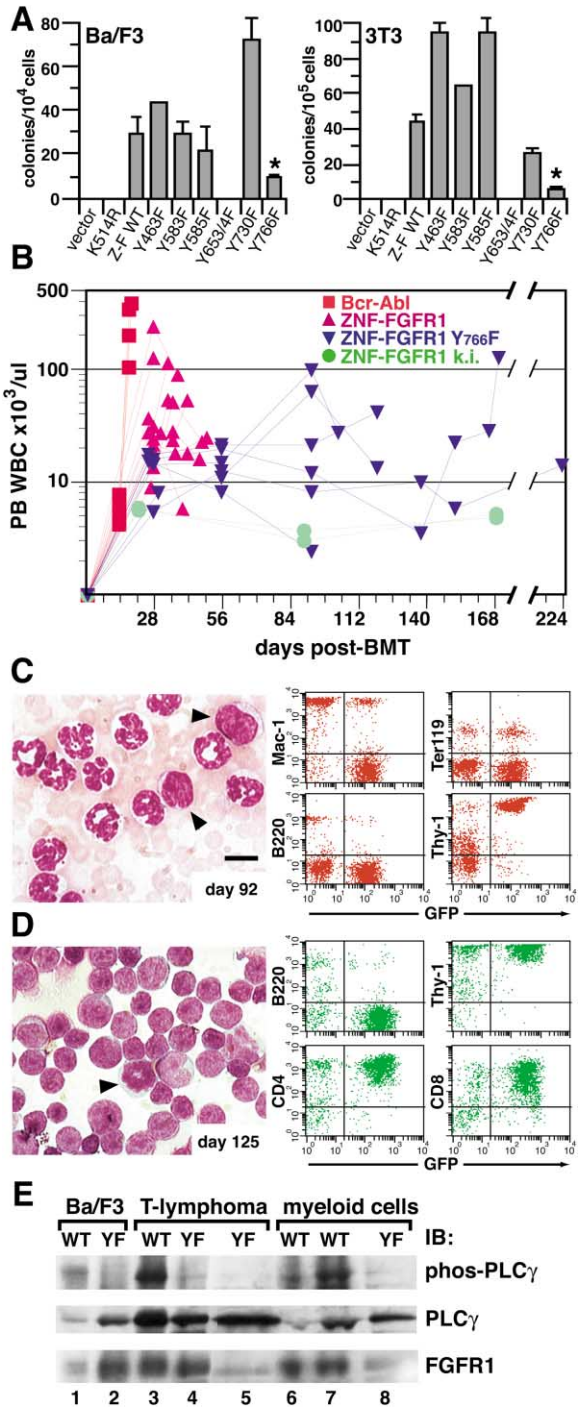

Figure 4. The PLC-γ1 binding site at FGFR1 Tyr766 contributes to ZNF198-FGFR1-induced transformation and leukemogenesis

A: In vitro transformation. The ability of *ZNF198-FGFR1* mutants to induce IL-3- and anchorage-independent growth in Ba/F3 (left panel) and NIH 3T3 (right panel) cells was determined in a stringent single-step transformation assay (see Experimental Procedures). Results (mean + SEM) are representative of three independent experiments; the difference in colony number for the Y766F mutant (asterisks) versus wild-type (Z-F WT) was statistically significant in both cell types ($p \leq 0.05$, unpaired *t* test), while none of the other mutants was significantly different. Vector = MIG virus without an oncogene insert.

B: Plot of peripheral blood leukocyte count (*y* axis, logarithmic scale) versus time after transplantation (*x* axis) for the recipients in Figure 1B (red squares, *BCR-ABL*: upright magenta triangles, *ZNF198-FGFR1*; inverted blue triangles, *ZNF198-FGFR1* Y766F; green circles, kinase-inactive (K514R) *ZNF198-FGFR1*). Most *ZNF198-FGFR1* Y766F recipients exhibited attenuated MPD with leukocyte counts of 10–25 × $10^3/\mu l$ during the first two months posttransplantation.

C: Wright-Giemsa stain (left panel) and flow cytometric analysis (right panels) of peripheral blood from a recipient of *ZNF198-FGFR1* Y766F-transduced marrow at 92 days posttransplant, with leukocyte count of 63.0 × $10^3/\mu l$. Note the predominance of neutrophils with several immature circulating lymphoblasts (arrowheads).

D: Wright-Giemsa-stained cytospin preparation (left panel) and flow cytometric analysis (right panels) of malignant lymph node cells from the mouse in **C** at time of sacrifice 125 days posttransplant. Note the uniform population of small to medium-sized lymphoblasts and mitotic figure (arrowhead).

In **C** and **D**, normal cells stained with isotype control antibody were >99% in the left lower quadrant (data not shown). Scale bar: 10 μm (**C** and **D**).

E: PLC-γ1 phosphorylation in Ba/F3 cells and primary leukemia cells from diseased mice. Membrane with protein extracts from Ba/F3 cells (lanes 1–2) or primary malignant T lymphoma (lanes 3–5) or myeloid cells (lanes 6–8) from diseased mice expressing ZNF198-FGFR1 wild-type (WT, lanes 1, 3, 6, and 7) or ZNF198-FGFR1 Y766F (YF, lanes 2, 4, 5, and 8) was immunoblotted (IB) with antibodies against phospho-Tyr783 PLC-γ1 (top panel), total PLC-γ1 (middle panel), and FGFR1 (bottom panel; ZNF198-FGFR1 appears as multiple species due to glycosylation). In parallel studies, p210 Bcr-Abl did not induce phosphorylation of PLC-γ1 Tyr783 in Ba/F3 cells (data not shown). Lane 1 was underloaded as judged by Ponceau S staining, while decreased ZNF-FGFR1 Y766F expression in lanes 5 and 8 correlated with the proportion of GFP^+ cells in these samples (data not shown).

Bcr-FGFR1 but not ZNF198-FGFR1 binds directly to Grb2 via Bcr Tyr177

Bcr-Abl binds directly to the SH2 domain of the adaptor protein Grb2 via a phosphorylated Tyr177 site in Bcr, and mutation of Tyr177 to Phe severely attenuates *BCR-ABL*-induced MPD in mice (Million and Van Etten, 2000). Whereas FGFR1 can bind Grb2 indirectly via the FRS2/SNT-1 adaptor protein, the ZNF198-FGFR1 fusion protein lacks the juxtamembrane FRS2 binding site (Ong et al., 2000). In coimmunoprecipitation experiments, we demonstrated that ZNF198-FGFR1 did not bind Grb2, while Bcr-FGFR1 efficiently coprecipitated with Grb2 (Figure 5E). To determine whether Bcr Tyr177 was responsible, we generated a Bcr-FGFR1 Y177F mutant and found that the mutant fusion protein lacked any detectable interaction with Grb2 (Figure 5E). These results demonstrate that fusion of Bcr to FGFR1 permits this tyrosine kinase to bind directly to Grb2 through Tyr177.

The Grb2 binding site is required for induction of CML-like MPD by Bcr-FGFR1

To determine the role of the Grb2 binding site in leukemogenesis by Bcr-FGFR1, we expressed *BCR-FGFR1* Y177F in primary murine bone marrow followed by transplantation into secondary recipients. Relative to *BCR-FGFR1*, recipients of *BCR-FGFR1* Y177F-transduced marrow had significantly prolonged survival (Figure 5B and Table 1), developed lower and more stable leukocyte counts (Figure 5D), and ultimately succumbed to intestinal T lymphoma that was identical to that induced by *ZNF198-FGFR1* (data not shown). Loss of direct Grb2 binding therefore attenuates the CML-like disease induced by *BCR-FGFR1* to one closely resembling EMS-like disease of *ZNF198-FGFR1*. The histopathology of *BCR-FGFR1* Y177F-induced disease differed from both the CML-like and EMS-like syndromes by the presence of large infiltrates of malignant histiocytes in the livers of these recipients (Table 1 and data not shown). Bcr-FGFR1 fusion protein was expressed in malignant myeloid progenitors

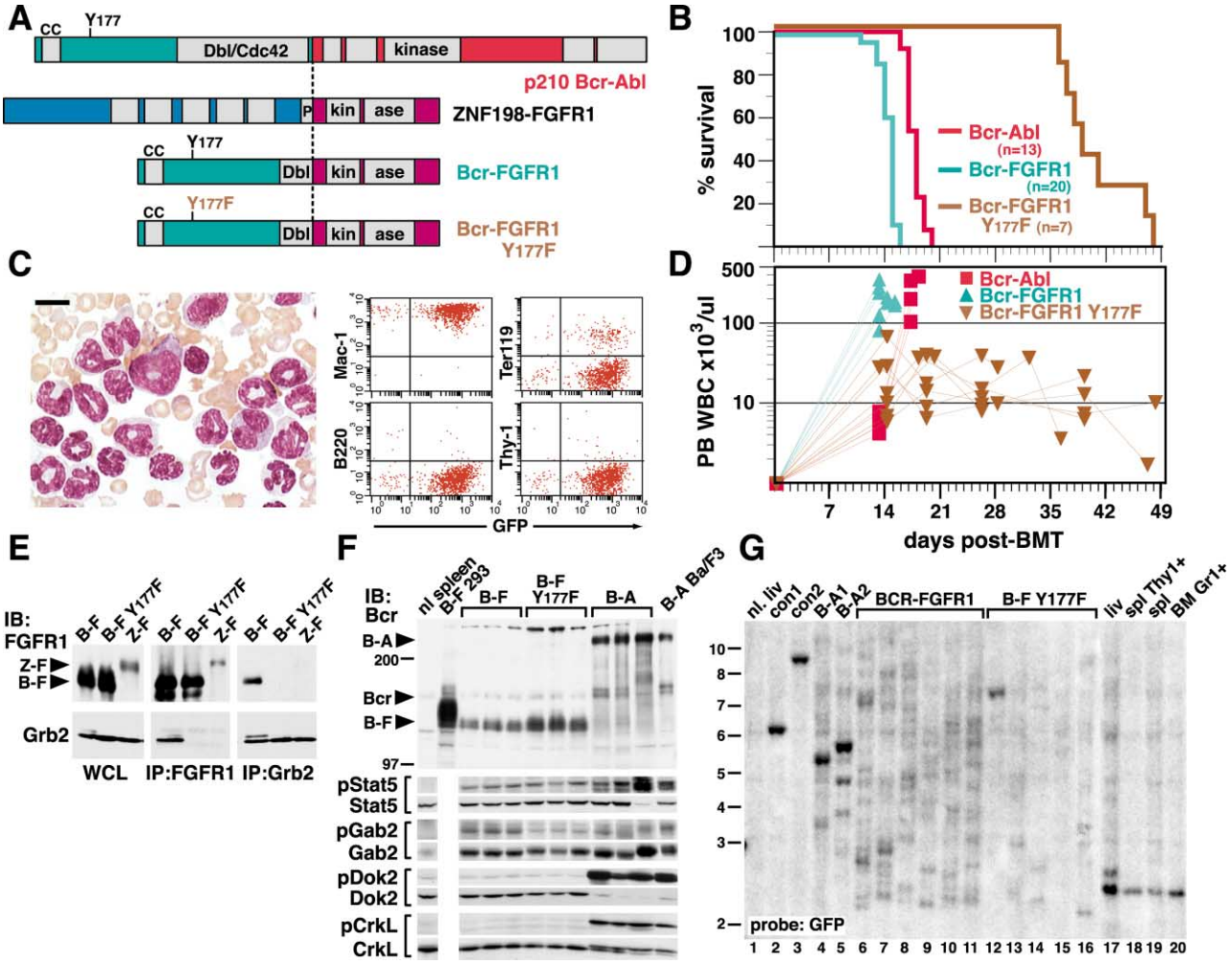

Figure 5. Rapidly fatal CML-like MPD induced in mice by *BCR-FGFR1* requires Bcr Tyr177

A: Schematic of (top to bottom) p210 Bcr-Abl, ZNF198-FGFR1, and Bcr-FGFR1 polypeptides, including the Bcr-FGFR1 Grb2 binding site mutant (Y177F). Domains indicated by gray boxes include the coiled-coil (CC) domain, Tyr177 Grb2 binding site, and Dbl/Cdc42 homology domain in Bcr, the kinase domain in Abl, MYM repeats and proline-rich (P) dimerization domain in ZNF198, and split kinase domain in FGFR1. The point of fusion is indicated by the vertical dotted line.

B: Survival curve for recipients of bone marrow transduced with *BCR-ABL* (red, n = 13), *BCR-FGFR1* (green, n = 20), and the *BCR-FGFR1* Y177F mutant (brown, n = 7). The difference in survival between any of the individual arms is highly significant ($p < 0.0001$, Mantel-Cox test).

C: Fulminant CML-like MPD induced by *BCR-FGFR1*. Wright-Giemsa stain (left panel) and flow cytometric plots (right panel) of peripheral blood of *BCR-FGFR1* recipient 14 days posttransplant with leukocyte count of 240 × 10^3/μl. Note the more immature circulating myeloid and erythroid progenitors, with predominantly GFP^+ Mac-1^+ cells. Scale bar: 10 μm.

D: Plot of peripheral blood leukocyte count (*y* axis, logarithmic scale) versus time after transplantation (*x* axis) for the recipients in **B** (red squares, *BCR-ABL*; upright green triangles, *BCR-FGFR1*; inverted brown triangles, *BCR-FGFR1* Y177F).

E: Grb2 binds Bcr-FGFR1 through Tyr177. Bcr-FGFR1 (B-F), Bcr-FGFR1 Y177F (B-F Y177F), or ZNF198-FGFR1 (Z-F) proteins were expressed in 293 cells and whole cell extracts (WCL, left) and anti-FGFR1 (middle) and anti-Grb2 (right) immunoprecipitates (IP) immunoblotted (IB) with anti-FGFR1 (top panels) or anti-Grb2 (bottom panels) antibodies. Note that Bcr-FGFR1, like Bcr-Abl (Li et al., 2001a), induces a lower mobility species of Grb2 that correlates with tyrosine phosphorylation.

F: Levels of Bcr-FGFR1, Bcr-FGFR1 Y177F, and Bcr-Abl fusion proteins and substrate phosphorylation in primary malignant myeloid progenitors from diseased mice. Lysates from peripheral blood samples (all >90% GFP^+ at the time of collection) from three different leukemic mice for each fusion protein were immunoblotted with antibodies against Bcr (top panel) or pairs of antibodies against Stat5, Gab2, Dok2, or CrkL and their respective tyrosine-phosphorylated forms (bottom panels). Note that high-level phosphorylation of Stat5 and Dok2 reduces detection of the protein by the pan-reactive antibody. All lanes were equally loaded as judged by Ponceau-S staining and levels of endogenous Bcr protein (arrowhead). Extracts from normal spleen (nl spleen) and control extracts from 293 cells expressing *BCR-FGFR1* (B-F 293) or Ba/F3 cells expressing *BCR-ABL* (B-A Ba/F3) are included. Positions of Bcr-FGFR1 (B-F) and Bcr-Abl (B-A) fusion proteins are indicated by arrowheads; molecular mass markers are on the left.

G: *BCR-FGFR1*-induced disease is polyclonal. Genomic DNA from spleens of mice with *BCR-FGFR1*-induced CML-like disease (lanes 6–11) or *BCR-FGFR1* Y177F-induced disease (lanes 12–16 and 19) was analyzed for proviral integrations as in Figure 3B. The first five control lanes on the left are as in Figure 3B. The lower intensity of the proviral bands from B-F Y177F samples correlated with the reduced frequency of GFP^+ cells in these samples (data not shown). Lanes 17–19 represent lineage analysis from a single B-F Y177F recipient (see text). Positions of DNA size markers (in kb) are to the left.

at slightly lower levels than Bcr-FGFR1 Y177F or Bcr-Abl (Figure 5F, top), demonstrating that the more aggressive MPD induced by Bcr-FGFR1 was not due to increased expression of this kinase. We analyzed phosphorylation of several substrates in the malignant cells using phospho-specific antibodies (Figure 5F, bottom). Stat5 and Gab2 were activated by both Bcr-Abl and Bcr-FGFR1. Phosphorylation of Stat5 was somewhat higher in Bcr-Abl-expressing cells, while efficient phosphorylation of Gab2 by Bcr-FGFR1 required Tyr177, as previously shown for Bcr-Abl (Sattler et al., 2002). However, Dok2 and CrkL were phosphorylated only by Bcr-Abl and were not appreciably activated in Bcr-FGFR1-expressing cells. In contrast to the oligoclonal *ZNF198-FGFR1*-induced EMS-like disease, the diseases induced by both *BCR-FGFR1* and the Y177F mutant were polyclonal, similar to *BCR-ABL*-induced leukemia (Figure 5G). In one *BCR-FGFR1* Y177F recipient (Figure 5G, lanes 17–20), the same proviral clones were observed in liver histiocytic sarcoma (liv), spleen T lymphoma (spl Thy1$^+$), and bone marrow neutrophils (BM Gr1$^+$), demonstrating a common origin from multipotential progenitors.

Discussion

If the future of cancer therapeutics lies in molecularly targeted drugs, a major focus will be on the identification, validation, and preclinical evaluation of candidate drug targets for the many different forms of cancer. Much interest has centered on dysregulated tyrosine kinases in leukemia because, by analogy with Bcr-Abl, they are attractive potential drug targets. In the murine retroviral bone marrow transduction/transplantation model, several dysregulated tyrosine kinases do not faithfully reproduce the human leukemia from which they were isolated. Tel-Jak2 induces simultaneous myelo- and lymphoproliferative disease in mice that is not observed in patients with t(9;12) (Schwaller et al., 1998). The NPM-ALK fusion protein induces diffuse large B cell lymphoma in mice but not the anaplastic lymphoma characteristic of t(2;5) non-Hodgkin's lymphoma patients (Kuefer et al., 1997). The FIP1L1-PDGFRA fusion kinase (Cools et al., 2003) induces MPD in mice, not the hypereosinophilic syndrome found in patients. In contrast, we demonstrated here that the *ZNF198-FGFR1* fusion oncogene of the (8;13) translocation induces hematologic disease in mice that very closely resembles human EMS. Recipients of *ZNF198-FGFR1*-transduced bone marrow uniformly develop MPD and T lymphoma that arises from a common hematopoietic stem/progenitor cell. Similar to patients with t(8;22), the *BCR-FGFR1* oncogene induced very rapid CML-like disease in the same mouse model system. Hence, the distinct human leukemia syndromes associated with these dysregulated tyrosine kinases are faithfully and accurately modeled in mice. Our results implicate the ZNF198-FGFR1 and Bcr-FGFR1 tyrosine kinases as the direct cause of their respective diseases and validate both as drug targets. Furthermore, while the reciprocal *FGFR1-ZNF198* fusion transcript is expressed in some patients with t(8;13) EMS disease (Popovici et al., 1998), our findings argue that neither the respective reciprocal translocation products nor haploidy for either the *ZNF198* or *FGFR1* genes are essential for leukemogenesis.

BCR-ABL and *BCR-FGFR1* induce polyclonal myeloproliferative disease in mice, which implies that the expression of the fusion kinase alone is sufficient to induce leukemia (Li et al., 1999). In contrast, the MPD induced by *ZNF198-FGFR1* was oligoclonal (Figure 3B), suggesting either that *ZNF198-FGFR1* alone is insufficient for disease induction, or alternatively that a restricted (and more primitive) population of hematopoietic stem/progenitor target cells is sensitive to transformation by *ZNF198-FGFR1*. Consistent with the latter model, only a small subset of the many *BCR-ABL*-transduced clones found in primary mice with CML-like disease are capable of self-renewal as measured by generation of CFU-S_{12} or propagation of leukemia upon secondary transplantation (Li et al., 1999), whereas the majority of *ZNF198-FGFR1*-transduced clones were transplantable (Figure 3G and data not shown). Further characterization of the stem cells initiating the two leukemias will be necessary to establish this hypothesis. On the other hand, *ZNF198-FGFR1* alone is not sufficient to induce T lymphoma. *ZNF198-FGFR1* perturbs but does not block thymocyte development, and mice with EMS-like disease have apparently normal CD4 and CD8 single positive *ZNF198-FGFR1*-expressing T cells in peripheral lymph nodes. Hence, in contrast to oncogenic transcription factors such as constitutively active Notch (Pear et al., 1996), a block in thymocyte differentiation is not a primary biological effect of *ZNF198-FGFR1* expression, and additional events, genetic and/or epigenetic, must contribute to the development of T lymphoma in these mice.

While the FGFR1 tyrosine kinase domain is an excellent drug target, monotherapy of EMS with an FGFR1 kinase inhibitor is likely to lead eventually to drug resistance, as is the case with imatinib for CML (Shah et al., 2002). Identification of the critical signaling pathways downstream of ZNF198-FGFR1 that contribute to leukemogenesis is important because simultaneous inhibition of these pathways may complement kinase inhibitor therapy. We initially focused on the role of FGFR1 autophosphorylation sites and used transformation of Ba/F3 and 3T3 cells as a surrogate assay to prioritize the selection of different autophosphorylation site mutants for leukemogenesis studies. Contrary to an initial report (Ollendorff et al., 1999) but in agreement with subsequent studies (Smedley et al., 1999; Xiao et al., 2000), we found wild-type *ZNF198-FGFR1* capable of inducing both IL-3-independent survival and proliferation of Ba/F3 cells. Although all kinase-active ZNF198-FGFR1 mutants induced proliferation of Ba/F3 cells in liquid culture (data not shown), in a stringent colony-forming assay, mutation of FGFR1 Tyr766 impaired transformation of Ba/F3 cells by *ZNF198-FGFR1*. The Y766F mutation has also been reported to abolish IL-3-independent survival of Ba/F3 cells and attenuate myeloproliferative disease induced by the related *FOP-FGFR1* fusion (Guasch et al., 2001, 2004). In FGF receptor-1, the Y766F mutation abolishes FGF-induced phosphaditylinositol hydrolysis but has no effect on mitogenesis (Mohammadi et al., 1992). However, FGF receptors that lack FRS2 association and activation are more dependent on Tyr766 for signaling (Lin et al., 1998), suggesting that the ZNF198-FGFR1 fusion protein may also rely on this site for generating oncogenic signals. In support of this hypothesis, the Y766F mutation significantly attenuated both the MPD and T lymphoma induced in mice by *ZNF198-FGFR1* and abolished activation of PLC-γ1 in primary leukemia cells by the fusion protein. The T lymphomas that eventually developed in *ZNF198-FGFR1* Y766F recipients had a more mature phenotype that is similar to those induced by *BCR-ABL* Y177F, and may arise from a distinct T lymphoid progenitor (Million and Van Etten, 2000). Our results identify PLC-γ1 and its downstream effectors including the protein kinase C family as additional

targets for therapy in EMS, and inhibitors of these enzymes can be tested, alone or in combination with FGFR1 inhibitors, in our model.

The Bcr-FGFR1 kinase binds Grb2 and induced fulminant CML-like MPD in recipient mice, demonstrating that the identity of the NH_2-terminal partner protein fused to FGFR1 can dramatically alter the leukemia phenotype. The Bcr Y177F mutation abolished Grb2 association and greatly attenuated the MPD induced by Bcr-FGFR1 to a more chronic illness resembling EMS, including intestinal T lymphoma. Direct binding of Grb2 to Bcr-FGFR1 therefore explains the aggressive CML-like disease induced by this fusion kinase. It has recently been shown that the Gab2 adaptor protein is recruited to Bcr-Abl Tyr177 through interaction with Grb2, which is required for efficient phosphorylation of Gab2 and for transformation of hematopoietic cells by Bcr-Abl through activation of the phosphatidylinositol 3-kinase and ERK/MAPK pathways (Sattler et al., 2002). Likewise, we found that activation of Gab2 by Bcr-FGFR1 required Tyr177, suggesting that Gab2 is probably the critical partner for Grb2 downstream of Bcr-FGFR1 as well as Bcr-Abl. As a corollary, our studies predict that Gab2 may be required for leukemogenesis by *BCR-FGFR1* but not *ZNF198-FGFR1*, and the availability of Gab2-deficient mice (Gu et al., 2001) will allow this hypothesis to be tested directly. The tyrosine kinase portion of the fusion protein can also influence leukemia signaling and phenotype. The signaling proteins Dok2 and CrkL were phosphorylated by Bcr-Abl but not Bcr-FGFR1, perhaps due to direct physical interactions with Abl (Druker et al., 1992; Ren et al., 1994), while PLC-γ1 was bound and activated by the FGFR1 fusion kinases but not Bcr-Abl. Previous studies with FOP-FGFR1 have also implicated the MAPK and Akt/mTOR pathways in transformation (Guasch et al., 2001). Intestinal T lymphoma is never observed in recipients of *BCR-ABL*-transduced marrow but is found in *BCR-FGFR1* Y177F recipients, suggesting that the FGFR1 kinase domain is required specifically for this disease, although identification of the precise signaling pathways involved will require further studies.

In conclusion, our results demonstrate that CML and EMS, distinct human leukemia syndromes associated with different fusion tyrosine kinases, are accurately and quantitatively modeled in mice and implicate different signaling pathways originating from both the kinase domain and the NH_2-terminal fusion partner in their pathogenesis. This model system should be valuable for further study of the molecular pathophysiology of EMS and for developing and testing targeted therapies for this disease.

Experimental procedures

DNA constructs

cDNAs for *ZNF198-FGFR1* (Reiter et al., 1998) and *BCR-FGFR1* (Demiroglu et al., 2001) were introduced into the EcoRI site of the MSCV-IRES/GFP (MIG) retroviral vector (Schwaller et al., 1998), allowing coexpression of the fusion tyrosine kinase and enhanced green fluorescent protein via an internal ribosome entry site. In ZNF198-FGFR1, Lys514 to Arg and Tyr to Phe mutations at positions 463, 583, 585, 653/654, 730, and 766 (amino acids are numbered according to their position in normal FGFR1) in FGFR1 were generated by PCR and confirmed by DNA sequencing.

Bone marrow transduction and transplantation

High-titer, replication-defective ecotropic retroviral stocks were generated by transient transfection of 293 cells using the *kat* system as described (Million et al., 2002), and titered by flow cytometric and genomic DNA Southern blot analysis of cells transduced with serial dilutions of virus. All viral stocks were matched for titer and gave equivalent transduction efficiency in 3T3 cells and primary murine bone marrow (data not shown). Bone marrow transduction and transplantation was carried out using 5-fluorouracil-treated (200 mg/kg) male donor and lethally irradiated (900 cGy) female recipient Balb/c mice (Taconic Farms, Germantown, Maryland) exactly as described (Li et al., 1999; Million et al., 2002). For secondary transplantation, 3×10^6 viable bone marrow cells or an equal mixture of marrow and splenocytes from primary diseased mice were transferred by tail vein injection into lethally irradiated Balb/c recipient mice.

Analysis of diseased mice

Premoribund mice were sacrificed and analyzed by cytospin and histopathology as described (Li et al., 1999; Million and Van Etten, 2000). For immunohistochemistry, tissues were embedded in OCT compound, frozen in 2-methylbutane, and cryostat sections fixed in acetone and stained with horseradish peroxidase (HRP)-conjugated monoclonal antibodies against Thy-1.2, CD4, CD8, B220, CD11b (all from Pharmingen, Carlsbad, California), TdT (Supertechs, Bethesda, Maryland), and GFP (Santa Cruz Biotechnology, Santa Cruz, California). HRP activity was detected by DAB reaction (DakoCytomation, Carpinteria, California) and sections counterstained with hematoxylin. For flow cytometry, cell populations were stained with PE-conjugated antibodies to hematopoietic cell surfaces antigens (all from Pharmingen) and analyzed on a FACScalibur flow cytometer (Becton Dickinson, Franklin Lakes, New Jersey). For analysis of T cell development, the GFP^+ $Thy1^+$ or GFP^+ $CD19^-$ $CD11b^-$ $CD8a^-$ populations from various tissues were costained with CD4-PE and CD8a-APC or CD25-PE and CD44-APC antibodies (Pharmingen), respectively.

Lineage and CFU-S_{12} analysis and Southern blotting

Purification of neutrophils and spleen erythroid progenitors and B lymphocytes employed lineage-specific monoclonal antibodies and magnetic beads (Miltenyi Biotec, Auburn, California), while peritoneal or bone marrow macrophages were isolated by adherence, as described (Li et al., 1999; Million et al., 2002). T lymphoma cells were obtained from mesenteric lymph nodes. The purity of the selected populations was assessed by Wright-Giemsa staining of cytospin preparations and in some cases by FACS analysis, and only those samples with $\geq$80% purity used for Southern blot analysis. Day 12 spleen colonies were isolated from secondary recipients of bone marrow from primary mice with ZNF198-FGFR1-induced disease as described (Million et al., 2002). Genomic DNA was prepared, digested with BglII, and hybridized with a radioactive probe from the *GFP* gene to detect distinct proviral integration events, then stripped and reprobed with a human *ZNF198* probe that detects a common 3.5 kb fragment from all proviruses and allows determination of total proviral content of each sample, as described (Li et al., 1999).

Ba/F3 and NIH3T3 cell transformation

Transformation of interleukin-3 (IL-3)-dependent Ba/F3 cells to IL-3-independent growth in soft agar and NIH 3T3 fibroblasts to anchorage-independent growth was performed essentially as described (Li et al., 2001a). Briefly, cells were transduced with retrovirus coexpressing ZNF198-FGFR1 or the indicated point mutants with GFP, cultured for 24 hr, then washed and plated in triplicate in 0.6% agar in medium with 10% serum but without supplemental growth factors. Colonies were counted 7 or 21 days later for Ba/F3 and 3T3 cells, respectively, and mean colony number normalized by the percentage of GFP^+ cells in the original transduced population as determined by flow cytometry (3%–10% for Ba/F3 cells and 30%–40% for 3T3 cells).

Western blotting and coimmunoprecipitation

Lysates from Ba/F3 cells stably expressing ZNF198-FGFR1 or the Y766F mutant were prepared in RIPA buffer while lysates from primary malignant T lymphoma or myeloid cells from diseased mice were prepared by direct boiling in sample buffer, then analyzed by SDS-PAGE and immunoblotting with polyclonal rabbit antibodies as described (Million et al., 2002). Antibodies specific for total and phospho-Tyr783 PLC-γ1, total and phospho-Tyr351 p56Dok2, phospho-Tyr207 CrkL, and phospho-Tyr452 Gab2 were obtained from Cell Signaling Technology (Beverly, Massachusetts), while antibodies to Bcr, FGFR1, Stat5, and CrkL were from Santa Cruz Biotechnology. Anti-

bodies against Gab2 were the kind gift of Dr. Haihua Gu (Beth Israel Deaconess Medical Center, Boston, Massachusetts). Coimmunoprecipitation of Grb2 and Bcr-FGFR1 was performed as described (Million and Van Etten, 2000).

Acknowledgments

We thank Dr. George Q. Daley for reagents and for critically reading the manuscript. This work was supported in part by NIH grants CA90576 and CA105043 (R.A.V.) and a SCOR grant from the Leukemia & Lymphoma Society. R.A.V. is a Stohlman Scholar of the Leukemia & Lymphoma Society.

Received: November 17, 2003
Revised: January 20, 2004
Accepted: February 3, 2004
Published: March 22, 2004

References

Cools, J., Stover, E.H., Boulton, C.L., Gotlib, J., Legare, R.D., Amaral, S.M., Curley, D.P., Duclos, N., Rowan, R., Kutok, J.L., et al. (2003). PKC412 overcomes resistance to imatinib in a murine model of FIP1L1-PDGFRα-induced myeloproliferative disease. Cancer Cell *3*, 459–469.

Daley, G.Q., Van Etten, R.A., and Baltimore, D. (1990). Induction of chronic myelogenous leukemia in mice by the P210$^{bcr/abl}$ gene of the Philadelphia chromosome. Science *247*, 824–830.

Demiroglu, A., Steer, E.J., Heath, C., Taylor, K., Bentley, M., Allen, S.L., Koduru, P., Brody, J.P., Hawson, G., Rodwell, R., et al. (2001). The t(8;22) in chronic myeloid leukemia fuses BCR to FGFR1: Transforming activity and specific inhibition of FGFR1 fusion proteins. Blood *98*, 3778–3783.

Druker, B., Okuda, K., Matulonis, U., Salgia, R., Roberts, T., and Griffin, J.D. (1992). Tyrosine phosphorylation of rasGAP and associated proteins in chronic myelogenous leukemia cell lines. Blood *79*, 2215–2220.

Fioretos, T., Panagopoulos, I., Lassen, C., Swedin, A., Billstrom, R., Isaksson, M., Strombeck, B., Olofsson, T., Mitelman, F., and Johansson, B. (2001). Fusion of the *BCR* and the fibroblast growth factor receptor-1 (*FGFR1*) genes as a result of t(8;22)(p11;q11) in a myeloproliferative disorder: The first fusion gene involving *BCR* but not *ABL*. Genes Chrom. Cancer *32*, 302–310.

Gu, H., Saito, K., Klaman, L.D., Shen, J., Fleming, T., Wang, Y., Pratt, J.C., Lin, G., Lim, B., Kinet, J.P., and Neel, B.G. (2001). Essential role for Gab2 in the allergic response. Nature *412*, 186–190.

Guasch, G., Mack, G.J., Popovici, C., Dastugue, N., Birnbaum, D., Rattner, J.B., and Pebusque, M.-J. (2000). FGFR1 is fused to the centrosome-associated protein CEP110 in the 8p12 stem cell myeloproliferative disorder with t(8;9)(p12;q33). Blood *95*, 1788–1796.

Guasch, G., Ollendorff, V., Borg, J.-P., Birnbaum, D., and Pebusque, M.-J. (2001). 8p12 stem cell myeloproliferative disorder: the FOP-fibroblast growth factor receptor 1 fusion protein of the t(6;8) translocation induces cell survival mediated by mitogen-activated protein kinase and phosphatidylinositol 3-kinase/Akt/mTOR pathways. Mol. Cell. Biol. *21*, 8129–8142.

Guasch, G., Popovici, C., Mugneret, F., Chaffanet, M., Pontarotti, P., Birnbaum, D., and Pebusque, M.-J. (2003). Endogenous retroviral sequence is fused to FGFR1 kinase in the 8p12 stem-cell myeloproliferative disorder with t(8;19)(p12;q13.3). Blood *101*, 286–288.

Guasch, G., Delaval, B., Arnoulet, C., Xie, M.J., Xerri, L., Sainty, D., Birnbaum, D., and Pebusque, M.J. (2004). FOP-FGFR1 tyrosine kinase, the product of a t(6;8) translocation, induces a fatal myeloproliferative disease in mice. Blood *103*, 309–312.

Inhorn, R.C., Aster, J.C., Roach, S.A., Slapak, C.A., Soiffer, R., Tantravahi, R., and Stone, R.M. (1995). A syndrome of lymphoblastic lymphoma, eosinophilia, and myeloid hyperplasia/malignancy associated with t(8;13)(p11;q11): description of a distinctive clinicopathological entity. Blood *85*, 1881–1887.

Kantarjian, H., Sawyers, C.L., Hochhaus, A., Guilhot, F., Schiffer, C., Gambacorti-Passerini, C., Niederwieser, D., Resta, D., Capdeville, R., Zoellner, U., et al. (2002). Hematologic and cytogenetic responses to imatinib mesylate in chronic myelogenous leukemia. N. Engl. J. Med. *346*, 645–652.

Kuefer, M.U., Look, A.T., Pulford, K., Behm, F.G., Pattengale, P.K., Mason, D.Y., and Morris, S.W. (1997). Retrovirus-mediated gene transfer of NPM-ALK causes lymphoid malignancy in mice. Blood *90*, 2901–2910.

Larsson, H., Klint, P., Landgren, E., and Claesson-Welsh, L. (1999). Fibroblast growth factor receptor-1-mediated endothelial cell proliferation is dependent on the Src homology (SH) 2/SH3 domain-containing adaptor protein Crk. J. Biol. Chem. *274*, 25726–25734.

Li, S., Ilaria, R.L., Million, R.P., Daley, G.Q., and Van Etten, R.A. (1999). The P190, P210, and P230 forms of the *BCR/ABL* oncogene induce a similar chronic myeloid leukemia-like syndrome in mice but have different lymphoid leukemogenic activity. J. Exp. Med. *189*, 1399–1412.

Li, S., Couvillon, A.D., Brasher, B.B., and Van Etten, R.A. (2001a). Tyrosine phosphorylation of Grb2 by Bcr/Abl and epidermal growth factor receptor: a novel regulatory mechanism for tyrosine kinase signaling. EMBO J. *20*, 6793–6804.

Li, S., Gillessen, S., Tomasson, M.H., Dranoff, G., Gilliland, D.G., and Van Etten, R.A. (2001b). Interleukin-3 and granulocyte-macrophage colony-stimulating factor are not required for induction of chronic myeloid leukemia-like myeloproliferative disease in mice by *BCR/ABL*. Blood *97*, 1442–1450.

Lin, H.-Y., Xu, J., Ischenko, I., Ornitz, D.M., Halegoua, S., and Hayman, M.J. (1998). Identification of the cytoplasmic regions of fibroblast growth factor (FGF) receptor 1 which play important roles in induction of neurite outgrowth in PC12 cells by FGF-1. Mol. Cell. Biol. *18*, 3762–3770.

Macdonald, D., Aguiar, R.C., Mason, P.J., Goldman, J.M., and Cross, N.C. (1995). A new myeloproliferative disorder associated with chromosomal translocations involving 8p11: A review. Leukemia *9*, 1628–1630.

Macdonald, D., Reiter, A., and Cross, N.C.P. (2002). The 8p11 myeloproliferative syndrome: A distinct clinical entity caused by constitutive activation of FGFR1. Acta Haematol. *107*, 101–107.

Million, R.P., and Van Etten, R.A. (2000). The Grb2 binding site is required for induction of chronic myeloid leukemia-like disease in mice by the Bcr/Abl tyrosine kinase. Blood *96*, 664–670.

Million, R.P., Aster, J., Gilliland, D.G., and Van Etten, R.A. (2002). The Tel-Abl (ETV6-Abl) tyrosine kinase, product of complex (9;12) translocations in human leukemia, induces distinct myeloproliferative disease in mice. Blood *99*, 4568–4577.

Mohammadi, M., Dionne, C.A., Li, W., Li, N., Spivak, T., Honegger, A.M., Jaye, M., and Schlessinger, J. (1992). Point mutation in FGF receptor eliminates phosphatidylinositol hydrolysis without affecting mitogenesis. Nature *358*, 681–684.

Mohammadi, M., Dikic, I., Sorokin, A., Burgess, W.H., Jaye, M., and Schlessinger, J. (1996). Identification of six novel autophosphorylation sites on fibroblast growth factor receptor 1 and elucidation of their importance in receptor activation and signal transduction. Mol. Cell. Biol. *16*, 977–989.

Ollendorff, V., Guasch, G., Isnardon, D., Galindo, R., Birnbaum, D., and Pebusque, M.-J. (1999). Characterization of FIM-FGFR1, the fusion product of the myeloproliferative disorder-associated t(8;13) translocation. J. Biol. Chem. *274*, 26922–26930.

Ong, S.H., Guy, G.R., Hadari, Y.R., Laks, S., Gotoh, N., Schlessinger, J., and Lax, I. (2000). FRS2 proteins recruit intracellular signaling pathways by binding to diverse targets on fibroblast growth factor and nerve growth factor receptors. Mol. Cell. Biol. *20*, 979–989.

Pear, W.S., Aster, J.C., Scott, M.L., Hasserjian, R.P., Soffer, B., Sklar, J., and Baltimore, D. (1996). Exclusive development of T cell neoplasms in mice transplanted with bone marrow expressing activated notch alleles. J. Exp. Med. *183*, 2283–2291.

Popovici, C., Adelaide, J., Ollendorff, V., Chaffanet, M., Guasch, G., Jacrot, M., Leroux, D., Birnbaum, D., and Pebusque, M.-J. (1998). Fibroblast growth factor receptor 1 is fused to FIM in stem-cell myeloproliferative disorder with t(8;13)(p12;q12). Proc. Natl. Acad. Sci. USA *95*, 5712–5717.

Popovici, C., Zhang, B., Gregoire, M.J., Jonveaux, P., Lafage-Pochitaloff, M., Birnbaum, D., and Pebusque, M.-J. (1999). The t(6;8)(q27;p11) transloca-

tion in a stem cell myeloproliferative disorder fuses a novel gene, FOP, to fibroblast growth factor receptor 1. Blood *93*, 1381–1389.

Reiter, A., Sohal, J., Kulkarni, S., Chase, A., Macdonald, D.H.C., Aguiar, R.C.T., Goncalves, C., Hernandez, J.M., Jennings, B.A., Goldman, J.M., and Cross, N.C.P. (1998). Consistent fusion of ZNF198 to the fibroblast growth factor receptor-1 in the t(8;13)(p11;q12) myeloproliferative syndrome. Blood *92*, 1735–1742.

Ren, R., Zheng, S.Y., and Baltimore, D. (1994). Abl protein-tyrosine kinase selects the Crk adapter as a substrate using SH3-binding sites. Genes Dev. *8*, 783–795.

Sattler, M., Mohi, M.G., Pride, Y.B., Quinnan, L.R., Malouf, N.A., Podar, K., Gesbert, F., Iwasaki, H., Li, S., Van Etten, R.A., et al. (2002). Essential role for Gab2 in transformation by BCR/ABL. Cancer Cell *1*, 479–492.

Schwaller, J., Frantsve, J., Aster, J., Williams, I.R., Tomasson, M.H., Ross, T.S., Van Rompey, L., Peeters, P., Van Etten, R.A., Ilaria, R., Jr., et al. (1998). Transformation of hematopoietic cell lines to growth-factor independence and induction of a fatal myeloid- and lymphoproliferative disease in mice by retrovirally transduced *TEL/JAK2* fusion gene. EMBO J. *17*, 5321–5333.

Shah, N.P., Nicoll, J.M., Nagar, B., Gorre, M.E., Paquette, R.L., Kuriyan, J., and Sawyers, C.L. (2002). Multiple BCR-ABL kinase domain mutations confer polyclonal resistance to the tyrosine kinase imatinib (STI571) in chronic phase and blast crisis chronic myeloid leukemia. Cancer Cell *2*, 117–125.

Smedley, D., Hamoudi, R., Clark, J., Warren, W., Abdul-Rauf, M., Somers, G., Venter, D., Fagan, K., Cooper, C., and Shipley, J. (1998). The t(8;13)(p11;q11–12) rearrangement associated with an atypical myeloproliferative disorder fuses the fibroblast growth factor receptor 1 gene to a novel gene *RAMP*. Hum. Mol. Genet. *7*, 637–642.

Smedley, D., Demiroglu, A., Abdul-Rauf, M., Heath, C., Cooper, C., Shipley, J., and Cross, N.C.P. (1999). ZNF198-FGFR1 transforms Ba/F3 cells to growth factor independence and results in high level tyrosine phosphorylation of STATs 1 and 5. Neoplasia *1*, 349–355.

Xiao, S., Nalabolu, S.R., Aster, J.C., Ma, J., Abruzzo, L., Jaffe, E.S., Stone, R., Weissman, S.M., Hudson, T.J., and Fletcher, J.A. (1998). *FGFR1* is fused with a novel zinc-finger gene, *ZNF198*, in the t(8;13) leukaemia/lymphoma syndrome. Nat. Genet. *18*, 84–87.

Xiao, S., McCarthy, J.G., and Fletcher, J.A. (2000). ZNF198-FGFR1 transforming activity depends on a novel proline-rich ZNF198 oligomerization domain. Blood *96*, 699–704.